# Elucidating the Association of Water in Wet 1-Octanol from Normal to High Temperature by Near- and Mid-Infrared Spectroscopy

**Francesca Palombo,[†] Thierry Tassaing,*[,‡,§] Marco Paolantoni,*[,†] Paola Sassi,[†] and Assunta Morresi[†]**

*Dipartimento di Chimica, Università degli Studi di Perugia, Via Elce di Sotto 8, I-06123 Perugia, Italy, Institut des Sciences Moléculaires, Groupe Spectroscopie Moléculaire, CNRS, UMR 5255, 351, Cours de la Libération, F-33405, Talence Cedex, France, and Institut des Sciences Moléculaires, Groupe Spectroscopie Moléculaire, Université de Bordeaux, UMR 5255, 351, Cours de la Libération, F-33405, Talence Cedex, France*

*Received: February 1, 2010; Revised Manuscript Received: May 14, 2010*

Near- (NIR) and mid-infrared (MIR) absorption spectra of pure and water-saturated 1-octanol were measured along the liquid−gas coexistence curve from ambient temperature and pressure up to 300 °C and 10 MPa. Density of the mixture as a function of temperature was assessed by spectral analysis in the NIR region. Two distinct regimes of temperature were identified in the evolution of solvent-subtracted spectra: at normal conditions and up to 180 °C, water is organized in multimeric H-bonded aggregates, while at higher temperature, mainly dimers and monomers exist. Water−water and alcohol−alcohol H-bonding interactions play a major role in wet octanol at low temperature, with resulting microheterogeneity and water segregation at a molecular level; on the other hand, water−alcohol interactions are relevant at higher temperature, as also revealed by the estimated density. At low temperature, water dissolved in octanol shows features which are comparable to those of interfacial water obtained by vibrational sum frequency (VSF) spectroscopy, while at high temperature the spectra generally reproduce those of water in the supercritical phase. Overall spectral assignment was supported by ab initio calculations at the MP2 level on small water clusters.

## 1. Introduction

The octanol−water partitioning system has become the standard reference for investigating the distribution characteristics of drugs between membranes and body fluids. Indeed, this system provides a surprisingly good correlation with water−membrane partitioning.[1,2] Thus, fundamental knowledge about the physical−chemical properties of wet octanol is needed for understanding the different mechanisms involved in these solvation processes. Liquid 1-octanol and its mixture with water have been investigated by using both experimental and theoretical methods with the aim of elucidating their molecular-level structure and dynamical aspects. Computer simulation studies[3–6] have provided a detailed characterization of the internal microstructure, hydrogen bonding (H-bonding), hydrophobic effect, polar/nonpolar clustering, and dynamics in both neat and water-saturated phases. The structure of the two systems is complex, and characterized by fluctuating regions of polar (hydroxyl groups) and nonpolar character (alkyl tails) that form elongated inverse micelles. These structures are believed to become larger and more spherical upon addition of water.[5] In a detailed Monte Carlo simulation work,[6] Chen and Siepmann have shown the incomplete mixing of water and octanol at a molecular level (due to the amphiphilic nature of the alcohol), yet evidencing that cylindrical micelle-like aggregates with a water core dominate in wet octanol. Thus, water may affect the structure of octanol,[5,6] although the hydration-related changes are thought not to be strong[5,6] and with a nonlocal character.[6] From an experimental point of view, neat 1-octanol has been the subject of a number of studies, using thermodynamic measurements,[7] X-ray diffraction,[8,9] near-infrared (with 2D correlation analysis),[10] Rayleigh−Brillouin,[11] Raman and infrared[12,13] spectroscopy, aimed at understanding its structure and dynamics under ambient conditions. It is generally accepted that chain-like H-bonded oligomers exist in the pure alcohol,[10–13] and this finding is consistent with computer simulation results.[5,6] The situation is less clear about the hydrated octanol. Direct structural information has been provided by X-ray diffraction experiments,[8,9] which show that the overall organization of 1-octanol is essentially preserved after addition of water. Besides, a study by Sassi et al.[14] using Brillouin, depolarized Rayleigh and Raman scattering spectroscopy has revealed no significant change in the structural and dynamical properties of liquid octanol upon water addition. It has then been inferred that alcohol−water H-bond interactions are probably not preferred compared to alcohol−alcohol and water−water ones,[5,15] and that hydrating water has only a minor effect on the octanol local environments, which are effectively stabilized by unaffected hydrophobic interactions. Previously observed modifications[6] are probably too small and/or too collective to be detected by employed spectroscopic techniques.[14] An NMR study[16] has shown that in wet octanol, hydrating water causes only a slight increase of the distance between alkyl chains of octanol molecules. Instead, an increase of hydrophobic interactions due to hydrating water has been revealed in concentrated *tert*-butanol mixtures.[17,18]

In a preliminary work,[14] Raman spectra have been interpreted by referring to the state of water in wet octanol as a distribution of "water pockets", similarly to the case of solutions of smaller alcohols.[17–21] A microscopic-level segregation of water in octanol

* To whom correspondence should be addressed. M.P.: E-mail: marcopa@unipg.it (M.P.) and t.tassaing@ism.u-bordeaux1.fr (T.T.).
† Università degli Studi di Perugia.
‡ Institut des Sciences Moléculaires, Groupe Spectroscopie Moléculaire, CNRS.
§ Institut des Sciences Moléculaires, Groupe Spectroscopie Moléculaire, Université de Bordeaux.

10.1021/jp1009548 
Published on Web 06/28/2010

has also been evidenced by using NMR,[16] and computer simulations[3–6] seem to confirm this depiction of the system. On the other hand, Monte Carlo simulations and small-angle X-ray scattering[22] reveal a spatially homogeneous distribution of water in primary alcohols (mainly near alcohol hydroxyls), while the existence of water pockets seems rather unlikely. Therefore, the central questions of the present study are as follows: May addition of water lead to a conspicuous reorganization of octanol? Do water molecules organize themselves forming water pockets in which water−water interactions prevail (water segregation)? If so, what are the size and architecture of these clusters compared to the bulk?

Molecular segregation of water in different alcohol solutions is enhanced by decreasing the temperature and increasing the pressure.[20] Since H-bonded aggregates of water and alcohol exist even in (pure) supercritical phase,[23,24] further questions may arise: How does the overall organization in wet octanol evolve as a function of temperature? Does water segregation (or any preferential interaction) occur in the liquid phase at high temperature?

Recent computational studies[25–27] have focused on characterizing the water/1-octanol interface, and the prominent role of octanol−water H-bonds in determining the typical arrangements in this specific region has been pointed out. At the interface, molecules interact under reduced density conditions; hence, studying H-bonding association at high temperature (low density) could be helpful to verify the proposed picture.

In the present study, Fourier transform infrared (FTIR) spectroscopy in both NIR and MIR regions was used to investigate intermolecular interactions and the aggregation state of water in hydrated 1-octanol at ambient conditions and along the liquid−gas coexistence curve (up to $T = 300$ °C and $P = 10$ MPa). The temperature-related spectral changes due to a strong modulation of intermolecular interactions were analyzed, also using ab initio calculations, and relevant structural information obtained. The aggregation properties of hydrating water were examined also in comparison with data of surface water and water in the supercritical phase, and interesting correlations were evidenced between these systems.

## 2. Materials and Methods

**2.1. Materials.** Spectrograde 1-octanol (99.8% purity) was obtained from Fluka, and ultrapure water (18 MΩ·cm) from a Milli-Q system. 1-Octanol, highly hydrophobic, was dissolved in water (10 mL each) and the resulting mixture was stirred thoroughly in a glass flask. After separation of the two phases (a few hours was sufficient), the octanol-rich phase was collected and used in this study.

**2.2. Spectroscopy.** NIR spectra were acquired with use of a special stainless steel cell[28] with sapphire windows and a 3 mm path length. Sealing of the cell was achieved by applying the unsupported area principle. The windows were positioned on the surface of an inconel plug, with a graphite foil placed between each window and the plug. Flat graphite rings ensured the sealing between the plug and cell body. Owing to the strong absorption of water and alcohols in the OH-stretching region, MIR spectra were obtained with use of a special stainless steel cell with sapphire windows and a 20 $\mu$m path length, which was ensured by a copper spacer. Heating of the cell was performed with cartridge heaters disposed around the body of the cell. Two thermocouples (±2 °C accuracy) were applied, one for regulating the temperature of the cartridges and the other to measure the temperature of the sample. Before each measurement, the sample was transferred into the cell and slowly heated to the working temperature. Pressure increased during heating, hence a valve was used for regulating its growth and obtaining the desired value for each experiment. Absolute uncertainty in the measured pressure was ±0.1 MPa, and the relative error was ±0.3%.

Infrared absorption spectra were acquired with an FTIR spectrometer (Bio-Rad FTS-60A), with a large sample compartment containing the cell, and a DTGS (Deuterated Triglycine Sulfate) detector. Two different sources, i.e. globar and tungsten halogen lamp, and beamsplitters, i.e. KBr/Ge and quartz substrate, were used for the measurements over the regions of mid- and near-infrared, respectively. Biorad WinIR software was used for acquisition and manipulation of the data. An infrared spectrum was obtained by Fourier transformation of 50 interferograms. Spectra were measured over the ranges 400−6000 (MIR) and 3000−10 000 $cm^{-1}$ (NIR) at 2 $cm^{-1}$ resolution with a zero filling factor of 2. For all spectral measurements, a background obtained in the absence of a sample was measured.

In the present work, NIR and MIR spectra of neat and water-saturated 1-octanol were obtained as a function of the temperature from room conditions up to 300 °C (with a 30 °C step), at variable pressure in the range 0.4−10 MPa. Pressure in the cell was maintained slightly above the saturation pressure of water during the course of the experiment. This enabled measurements to be performed along the liquid−gas coexistence curve, while preventing the liquid-to-vapor phase transition. Note that critical pressure of water ($P_c = 22.1$ MPa) is greater by a degree of magnitude than that of 1-octanol ($P_c = 2.77$ MPa), while their critical temperatures are comparable ($T_c =$ 374 and 379 °C for water and 1-octanol, respectively).

The contribution of water to the measured spectra was examined by subtracting the spectrum of neat 1-octanol from that of water-saturated 1-octanol acquired at the same thermodynamic conditions. Spectral subtraction was performed on the NIR and MIR data sets with BioRad WinIR software. After a linear baseline correction, integral absorbance of the second overtone of antisymmetric CH stretching ($3\nu_{CH}$) of 1-octanol over the range 7600−9000 $cm^{-1}$ was used as a reference for normalization.[24] (Since the band shape and center frequency of the $3\nu_{CH}$ overtone only slightly change with the increase of temperature and pressure, the extinction coefficient of this band was assumed to be independent of thermodynamic conditions applied.) The CH-stretching band of 1-octanol (in the MIR region) was unsuitable for normalization; hence, prior to subtraction each MIR spectrum was normalized by using the integrated absorbance of the $3\nu_{CH}$ band in the NIR spectrum acquired at the same experimental conditions.

The bands analyzed were the main water absorptions in the MIR and NIR spectral regions, i.e., the fundamental OH stretching in the range of 3000−3800 $cm^{-1}$, the HOH-bending + OH-stretching combination at approximately 5200 $cm^{-1}$, and the first overtone of OH stretching in the 6200−7700 $cm^{-1}$ range. (Note that vibrational modes of monomeric water are commonly denoted as $\nu_2$: bending; $\nu_1$: symmetric stretching; $\nu_3$: antisymmetric stretching.) Corresponding bands of 1-octanol are observed at similar wavenumbers, with the exception of the OH-bending + stretching ($\delta_{OH} + \nu_{OH}$) combination at approximately 4800 $cm^{-1}$. Pure 1-octanol spectra acquired at comparable thermodynamic conditions have been discussed in a previous work.[24]

Quantum chemistry calculations of small water clusters such as linear dimer, cyclic trimer, and cyclic tetramer were performed at the MP2/aug-cc-pVDZ level with Gaussian 03

software,[29] and the harmonic frequencies with corresponding IR and Raman intensities of OH-stretching modes were obtained accordingly to the works by Xantheas et al.[30,31]

**2.3. Density.** To our knowledge, the phase diagram of the water−1-octanol mixture has not been published, and related thermodynamic data are generally lacking. Here, we applied a method based on spectral analysis to obtain the density of water-saturated 1-octanol as a function of temperature along the liquid−gas coexistence curve.[32] Density of the solution can be expressed by the equation:

$$\rho = C_{oct}\left[M_{oct} + M_{wat}\left(\frac{1}{x_{oct}} - 1\right)\right] \quad (1)$$

where $M_{oct}$ and $M_{wat}$ are the molecular weights of 1-octanol (130 Da) and water (18 Da); $C_{oct}$ and $x_{oct}$ are the concentration and mole fraction of 1-octanol in the solution, respectively. At a first approximation, $x_{oct}$ can be considered constant with the temperature; the value of $x_{oct} = 0.74$ arose from estimation of the water mole fraction ($x_{wat} = 0.26$) at ambient conditions, using the experimental density of the mixture[14] and partial molar volumes of the components.[33] Hence, $C_{oct}$ is the only parameter showing a temperature dependence in eq 1. To obtain the plot of $C_{oct}$ as a function of temperature along the liquid−gas boundary curve, the $3\nu_{CH}$ overtone of 1-octanol used for spectral normalization was selected. At each temperature of the experiment, the ratio of integrated absorbance between the $3\nu_{CH}$ band in the spectrum of the mixture and that in the spectrum of neat 1-octanol was calculated. According to the Beer−Lambert law, and assuming that the absorption coefficient of this mode is almost pressure and temperature independent, this ratio is directly related to a concentration ratio. Therefore, at each temperature of the experiment, $C_{oct}$ (to be applied in eq 1) was calculated by using the concentration value of pure 1-octanol.[34]

Density estimated with the method of band integration was compared with that obtained for an ideal mixture of water and 1-octanol, by considering the volume of the mixture as a sum of volumes of the pure compounds, $V_m = x_{oct} \cdot V_{m,oct} + x_{wat} \cdot V_{m,wat}$ (wherein $V_m$ is the molar volume of the mixture). For the different temperatures of the experiment, the molar volumes of octanol ($V_{m,oct}$) and water ($V_{m,wat}$) were obtained from the literature.[34,35]

The density of the water-saturated 1-octanol was also measured at normal liquid conditions, in the range of $T = 5-70$ °C (ambient pressure), using an Anton Paar DMA 60 density meter (Graz, Austria), to which was attached an external measuring cell (type DMA 512P), having an accuracy of $1 \times 10^{-5}$ g·cm$^{-3}$. The temperature of the cell was controlled through a circulating water bath Haake F6, with a precision of ±0.1 °C.

## 3. Results and Discussion

**3.1. Estimation of Density.** Figure 1 shows the evolution of density of the water−1-octanol solution as a function of temperature along the liquid−gas coexistence curve, obtained by applying spectral data and eq 1. The density calculated in the ideal approximation and that measured at normal liquid conditions are also presented for comparison. At the lowest temperatures of the experiment, density obtained by the spectroscopic method reproduces the experimental value (differences are within the error bars), indicating the reliability of the applied procedure. Interestingly, the density obtained at the different temperatures in the investigated range is comparable

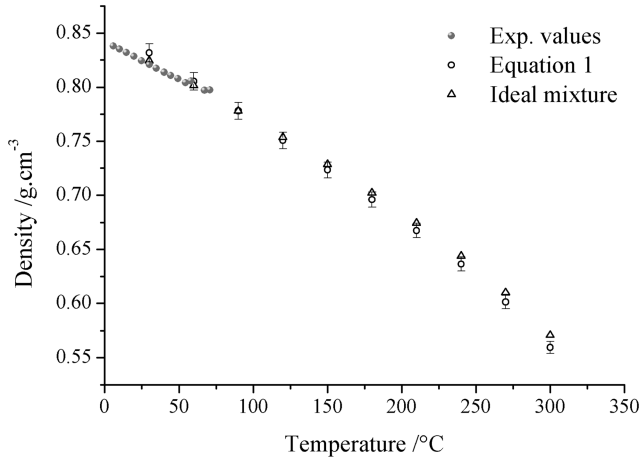


**Figure 1.** Plots of density of the water-saturated 1-octanol as a function of temperature, in the range of $T = 30-300$ °C along the liquid−gas coexistence curve: (empty circles) values obtained by applying eq 1 (see text; error bars: ±1%), (empty triangles) values calculated for an ideal mixture, and (filled circles) experimental values (at ambient pressure).

to that estimated within the hypothesis of an ideal mixture. This indicates that the concept of 1-octanol molar volume being essentially unchanged from the pure liquid to the water-saturated solution[14,33] can be extended from normal to more drastic thermodynamic conditions. Note that a slightly negative excess molar volume of the mixture at normal conditions has previously been obtained with use of high precision density measurements.[36,37] Our measurements do not allow us to appreciate such small effects, and the differences observed in Figure 1 at lower temperature are within the experimental precision. The ideal and estimated density show a perfect coincidence at $T =$ 90 °C. For higher temperature, the estimated value is slightly lower than the ideal one, with their difference becoming significant only at $T = 300$ °C. These results demonstrate that the excess volume of mixing, slightly negative at normal conditions,[36,37] becomes positive at higher temperature. The change in molar volume of mixing upon temperature variation has recently been reported for the ethanol−water system,[38] showing positive excess values under near-critical water conditions.

**3.2. Near-Infrared Spectra.** Figure 2 shows the evolution of the NIR spectrum of liquid 1-octanol and its water-saturated solution as a function of temperature along the liquid−gas coexistence curve. Changes are clearly observed for the bands of 1-octanol in the ranges 4500−5200 ($\delta_{OH} + \nu_{OH}$) and 6000−7500 cm$^{-1}$ ($2\nu_{OH}$) (Figure 2a), as well as for the combination band of water in the 5000−5600 cm$^{-1}$ range (Figure 2b). A contribution of water to the spectral absorbance is also detected in the region of the $2\nu_{OH}$ overtone, between ca. 6500 and 7500 cm$^{-1}$. In each spectral region the spectral profiles redistribute toward higher frequencies as the temperature increases. Since the formation of H-bonds between OH groups causes a decrease of the OH-stretching frequency, the observed changes may correlate with a reduced aggregation occurring at higher temperature (see also spectra of neat 1-octanol in ref 24). To better identify the effects of water addition to liquid octanol, difference profiles in the region between 4500 and 9000 cm$^{-1}$ were calculated according to the method described in Section 2, and displayed in Figure 3. The almost complete disappearance of the $2\nu_{CH}$ overtone of 1-octanol, beyond the $3\nu_{CH}$ band, validates our subtraction method. Two main absorptions can be observed at approximately 5200 and 7000 cm$^{-1}$,

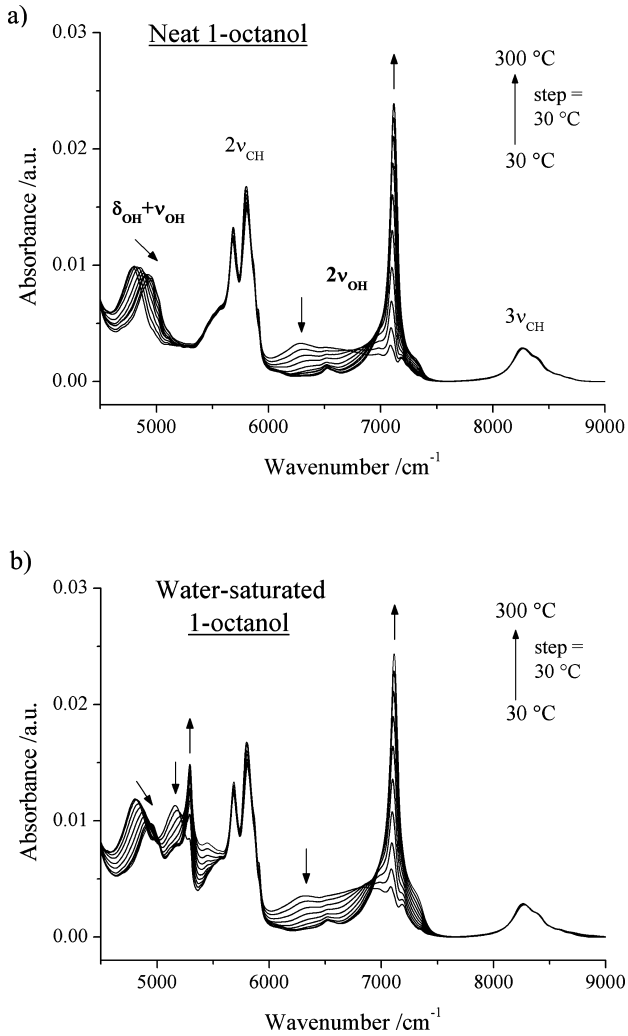


**Figure 2.** Evolution of the NIR spectra of (a) neat 1-octanol and (b) water-saturated 1-octanol as a function of temperature, in the range 30 to 300 °C along the liquid−gas coexistence curve. Spectra are normalized to the integrated absorbance of the $3\nu_{CH}$ band of octanol. (Arrows indicate the changes in absorbance of the bands in this spectral region.)

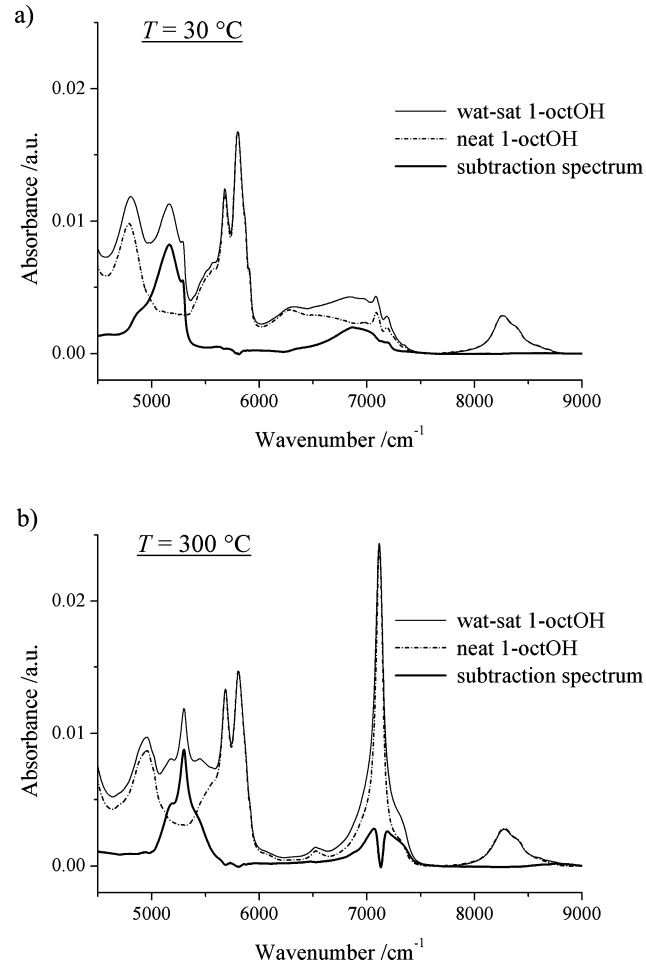


**Figure 3.** Normalized NIR spectra of neat 1-octanol (dash-dotted line) and water-saturated 1-octanol (thin line), along with the difference profile (thick line), at two selected temperatures: $T$ = 30 (a) and 300 °C (b).

corresponding to the $(\nu_2 + \nu_3)$ combination and $2\nu_{OH}$ overtone of water, respectively. Figure 4 shows the evolution of the profile in both regions as a function of the temperature. Difference spectra at near ambient conditions recall those obtained for butyl alcohol solutions.[39,40]

Relevant information can be obtained analyzing the combination band in Figure 4a. Owing to the minor contribution of 1-octanol absorbance in this spectral region, this band is particularly suitable for spectral analysis. The fraction of monomers and free OHs of water increases with the temperature, as indicated by a marked enhancement of the high-frequency spectral components. At lower temperature, essentially three components are detected, as previously observed with Raman spectroscopy.[14] The sharp signal at ca. 5290 cm$^{-1}$ can be assigned to the free OH of single-bonded water molecules (still involved in H-bonding by the other OH);[39−41] monomers become relevant only at intermediate to high temperatures. The prominent band at approximately 5200 cm$^{-1}$ can be related to the H-donor hydroxyl of water bonded through either one or both OHs. The shoulder at 4900 cm$^{-1}$ indicates the presence of strong H-bonds, which are typical of stable multimeric aggregates of water with a bulk-like structure.[14] Surprisingly, despite a low amount of water in the solution, the signature of strong water−water interactions persists up to $T$ = 120 °C.

At higher $T$, the main spectral feature is a structured profile with a maximum at 5300 cm$^{-1}$, which indicates the presence of monodispersed water.[42] The profile is attributed to the $(\nu_2 + \nu_3)$ combination of water monomers,[42] since it exhibits the PQR rovibrational structure typically observed for water in its gaseous and supercritical phases,[43] or highly diluted in hydrophobic solvents. Indeed similar spectra have been found for water dissolved in liquid $CCl_4$ and supercritical xenon,[44] as well as in supercritical $CO_2$.[42] The $(\nu_2 + \nu_1)$ combination mode, although less active in IR,[42] can give some intensity here. As will be discussed below, additional contributions arise from small aggregates such as water−water and water−alcohol dimers.

In the observed spectral evolution, two main association domains can thus be identified, respectively below and above some intermediate temperature around 180 °C: dissolved water evolves from a situation that can be described in terms of associated and free OHs (at lower $T$) toward a state dominated by monomers (at higher $T$).

The spectrum in the overtone region (Figure 4b) is more difficult to interpret. Besides water contributions, it also exhibits features due to hydration-related changes in the octanol H-bond structuring. Regarding the profile at low temperature, we can assign the band with a maximum at 6870 cm$^{-1}$, which decreases with the temperature increase, to the H-donor hydroxyl of water,[39,40] while the component near 7200 cm$^{-1}$, showing a

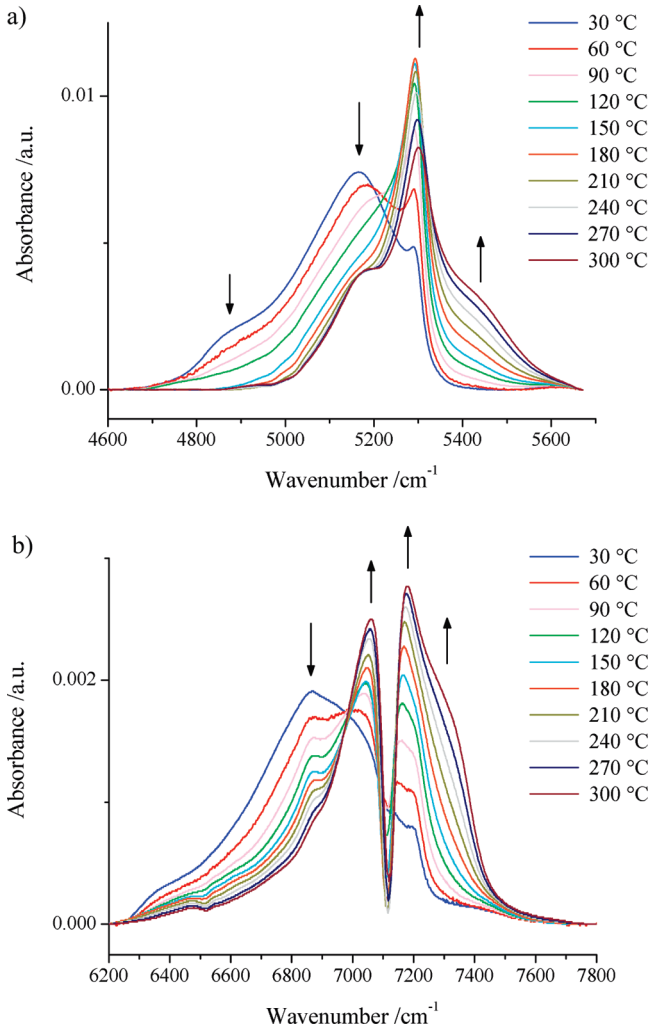


**Figure 4.** Evolution of the NIR difference spectrum in the regions of the water (a) combination band and (b) overtone as a function of temperature, in the range 30 to 300 °C along the liquid−gas coexistence curve.

simultaneous increase and broadening, can be assigned to the free (dangling) OH of single-bonded water.[39,40] The overall profile shifts to higher frequency with increasing temperature, while a strong minimum appears at 7100 $cm^{-1}$ indicating that the absorption due to the octanol free-OH signal in the spectra of the solution is lower than that in neat alcohol spectra. This finding reflects the relative decrease of 1-octanol free OHs in the solution compared to the neat alcohol. The fraction of nonbonded OHs in pure liquid 1-octanol has been found to vary from 0.5% to 6% at ambient conditions up to ca. 70% at $T$ = 300 °C and $\rho$ = 0.57 $g/cm^3$.[24] A large fraction of octanol free OHs is also revealed by the prominent band near 7200 $cm^{-1}$ in the spectrum of wet alcohol at high temperature (Figure 2b). Also, the symmetrical band shape suggests that, among the different contributions to this octanol signal,[41] monomeric hydroxyls must predominate over terminal H-acceptor OHs. Therefore, the minimum observed in the overtone region of the difference spectra can be related to the presence of octanol−water interactions with alcohol acting as H-donor. The relative signal decrease is nearly 15% indicating that at 300 °C, approximately 10% of all octanol molecules become H-donors in new octanol−water adducts. Since the solution contains water and octanol in the molecular ratio 1:2.8, it can be estimated that nearly 30% of water molecules in wet 1-octanol will be involved in this type of interactions. Notably, analogies are revealed with

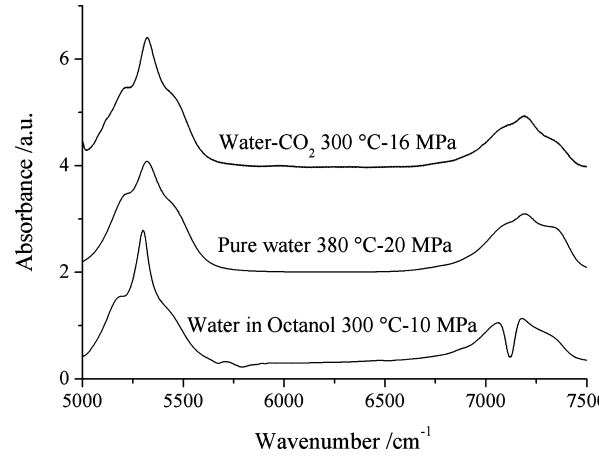


**Figure 5.** (Bottom to top) NIR spectrum of water in wet 1-octanol at $T$ = 300 °C and $P$ = 10 MPa, compared to that of supercritical water at $T$ = 380 °C and $P$ = 20 MPa,[43] and that of a binary water−$CO_2$ mixture ($CO_2$-rich phase) at $T$ = 300 °C and $P$ = 16 MPa.[42]

findings from calculations on water/1-octanol interfaces[27] (see below). Moreover, the free-OH peak of octanol in the solution is red-shifted (of ca. 3 $cm^{-1}$) with respect to that of pure alcohol. This means that slightly different environments of free-OH groups exist in the two systems, likely due to water−alcohol interactions in which octanol acts as H-acceptor.[41] Similarly to the signal change at 5400 $cm^{-1}$ (Figure 4a), an enhancement of absorbance at 7300 $cm^{-1}$ (Figure 4b) indicates the production of water monomers upon temperature increase.

In Figure 5, the difference spectrum obtained at the highest temperature of the experiment is compared with a spectrum of pure supercritical water (acquired at $T$ = 380 °C and $P$ = 20 MPa),[23,43] and with that of a water−$CO_2$ mixture ($CO_2$ rich phase) at $T$ = 300 °C and $P$ = 16 MPa.[42] In the combination region, the spectra exhibit comparable patterns of PQR rovibrational features indicating similar association properties of water in the three cases.[23,43] Note also the similarity among the spectra in the overtone region, except for the sharp minimum in the water-in-octanol profile (due to water−alcohol species). This finding demonstrates that in hydrated octanol, water monomers and dimers of both water−water and water−octanol types prevail over higher associates, which are present to a much lower degree.

**3.3. Mid-Infrared Spectra.** Figure 6 displays the evolution of the OH-stretching profile of pure and hydrated 1-octanol as a function of temperature along the liquid−gas coexistence curve. The temperature-induced breakage of large 1-octanol aggregates in both systems is indicated by both a decrease and blue-shift of the broad band with a maximum at 3350 $cm^{-1}$, due to bonded-OH groups. Simultaneously the fraction of octanol free OH increases, as indicated by a growth of absorbance at 3640 $cm^{-1}$. Dangling OHs of water in the solution give rise to a distinct signal at 3680 $cm^{-1}$ (see Figure 6b). Let us recall that the MIR spectrum is intrinsically more sensitive to H-bonding aggregation than the NIR one.[12,13] Figure 7 shows the difference spectra obtained subtracting the spectrum of pure octanol from that of water-saturated octanol at two selected temperatures. The evolution of the resulting profile as a function of temperature along the liquid−gas boundary is displayed in Figure 8.

At lower temperature than 180 °C, at least three spectral components are distinguished, consistently with corresponding NIR (Figure 4a) and Raman[14] profiles. Thus, we assign the component at 3200 $cm^{-1}$ to water multimers with strong H-bond

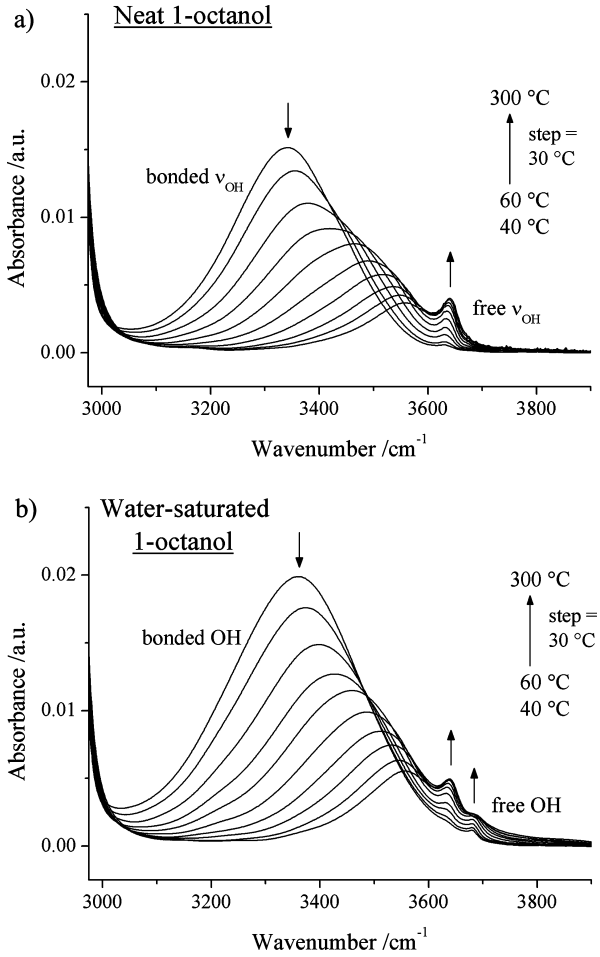


**Figure 6.** Evolution of the MIR spectrum of (a) neat 1-octanol and (b) water-saturated 1-octanol as a function of temperature, in the range 40 to 300 °C along the liquid−gas coexistence curve. Spectra are normalized to the integrated absorbance of the $3\nu_{CH}$ band in corresponding NIR spectra (see Figure 2). (Arrows indicate the changes in absorbance of the bands in this spectral region.)

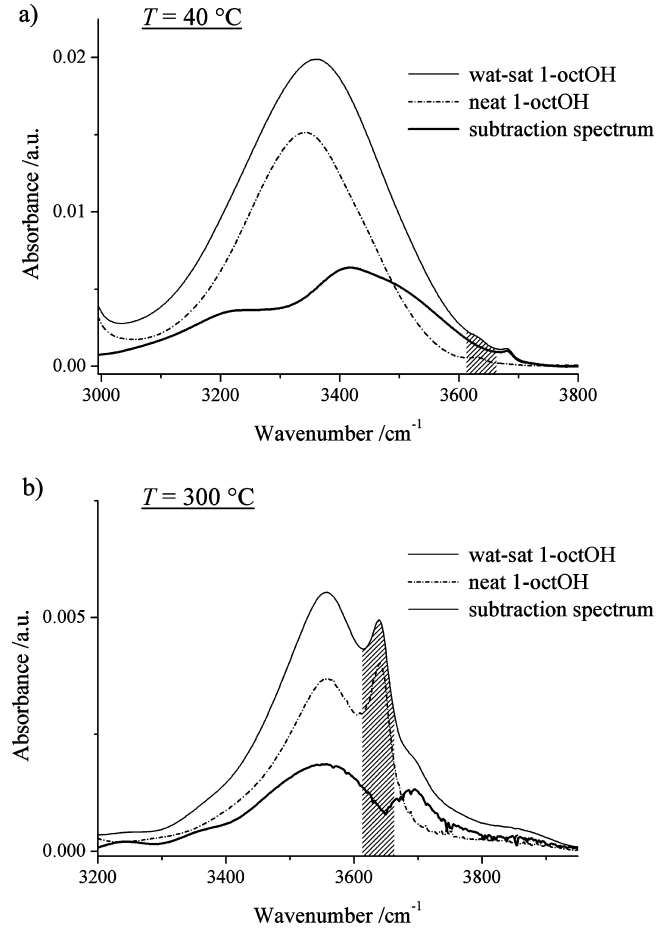


**Figure 7.** Normalized MIR spectra of neat 1-octanol (dash-dotted line) and water-saturated 1-octanol (thin line), along with the difference profile (thick line), at two selected temperatures: $T$ = 40 (a) and 300 °C (b). (Shaded areas indicate the free-OH signal of 1-octanol, which is removed after spectral subtraction.)

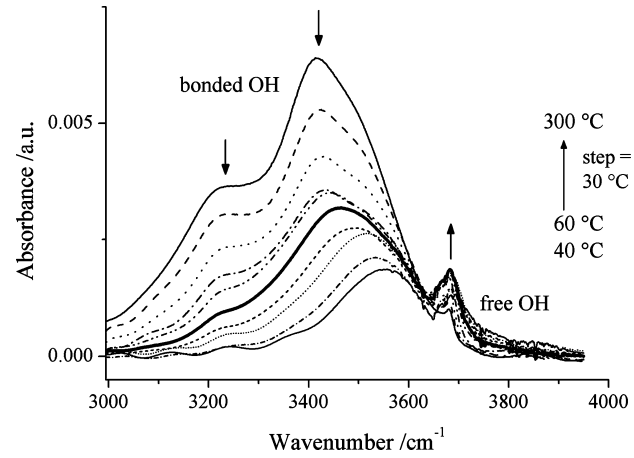


**Figure 8.** Evolution of the MIR difference spectrum in the region of the OH-stretching of water as a function of temperature, in the range 40 to 300 °C along the liquid−gas coexistence curve. (Arrows indicate the changes in absorbance of the bands in this spectral region. Thick line denotes the spectrum at $T$ = 180 °C, which exhibits the highest peak intensity of the free-OH signal.)

interactions. The low-frequency position and high Raman polarization[14] of this signal indicate that, same as for bulk water, it derives from the collective, symmetric stretching of coupled OHs within ordered (tetrahedral) clusters of water.[14,45] The band at approximately 3400 cm$^{-1}$ is instead attributed to water-bonded OHs which are characterized by weaker or distorted H-bonds. It also includes a contribution from single-bonded H-donor molecules (the other OH being free and absorbing at 3680 cm$^{-1}$). In analogy with spectra of pure water, the prominent features at 3200 and 3400 cm$^{-1}$ can thus be related to locally ordered and unordered water environments, respectively. The detection of a component at 3200 cm$^{-1}$ especially supports the view of molecular confinement for a consistent fraction of water in the solution.[6,14,18] Note that both these bands are narrower, and with the low-frequency one relatively less intense, than in bulk water. This can be explained considering that, while preventing the formation of extended ordered regions, the confinement of water reduces the inhomogeneous broadening of bonded-OH distributions.[14] Since the component at 3200 cm$^{-1}$ relates to low-energy low-density local domains,[45] its reduction compared with pure water may explain the negative value of excess volume[36,37] and the positive value of excess enthalpy previously reported.[37]

Figure 9 shows a MIR spectrum of water in 1-octanol and a polarized Raman spectrum of the same system, obtained at comparable temperature.[14] A similar OH-stretching pattern, with comparable peak positions between the two spectra, can be observed. This is especially remarkable for the signal at 3680 cm$^{-1}$, hence supporting its assignment to dangling OHs of single-bonded water. Indeed, water monomers give rise to IR and Raman spectra different from one another.[46] It is worth noting that, unlike pure water,[45,47] the relative intensity of the bands at 3200 and 3400 cm$^{-1}$ is similar between the IR and

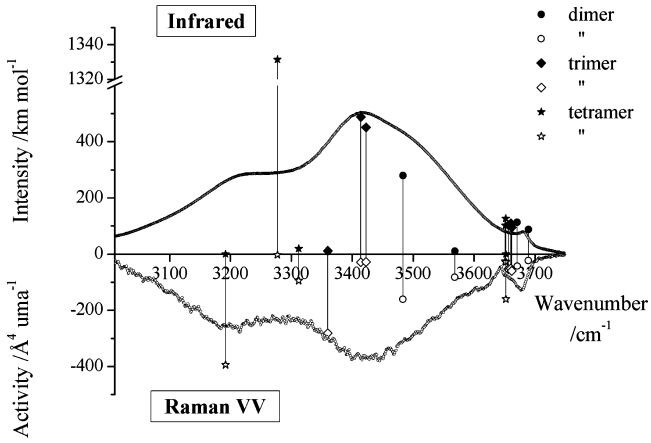


**Figure 9.** (Bottom and top) Polarized Raman[14] and MIR spectra of water in wet 1-octanol at $T = 35$ and 40 °C, respectively, both obtained by the subtraction method. Symbols with drop lines indicate the activity values of OH-stretching vibrations of small water clusters such as open dimers, closed trimers, and closed tetramers calculated at the MP2 level (see text).

**TABLE 1: Harmonic Frequency (Corrected for the 0.94 Factor[55]), IR Intensity, and Raman Activity of OH-Stretching Modes Obtained by MP2 Ab Initio Calculations of Linear Dimers, Cyclic Trimers, and Tetramers of Water**

| | | MP2/aug-cc-pVDZ | | |
|---|---|---|---|---|
| | | freq ($cm^{-1}$) | IR (km/mol) | Raman ($Å^4$/amu) |
| $(H_2O)_2$ | $\nu_{HB}$ | 3483.1517 | 279.7346 | 160.9943 |
| | $\nu_1$ | 3568.2174 | 10.2400 | 82.4968 |
| | $\nu_{free}$ | 3670.8469 | 113.4365 | 42.5303 |
| | $\nu_3$ | 3689.1400 | 88.0178 | 22.7827 |
| $(H_2O)_3$ | $\nu_{HB}$ | 3359.7170 | 11.3556 | 281.4365 |
| | | 3414.0555 | 487.6655 | 28.3472 |
| | | 3422.6207 | 450.6861 | 27.5230 |
| | $\nu_{free}$ | 3656.7158 | 103.7995 | 53.4534 |
| | | 3660.6493 | 110.0163 | 51.5043 |
| | | 3661.6757 | 95.1101 | 59.9004 |
| $(H_2O)_4$ | $\nu_{HB}$ | 3191.9044 | 0.0000 | 394.7688 |
| | | 3277.1435 | 1331.4829 | 2.5627 |
| | | 3277.1436 | 1331.4828 | 2.5627 |
| | | 3312.1415 | 19.2738 | 94.6621 |
| | $\nu_{free}$ | 3651.2060 | 101.4992 | 25.4175 |
| | | 3651.8669 | 126.1477 | 28.2707 |
| | | 3651.8669 | 126.1476 | 28.2707 |
| | | 3652.4296 | 0.0000 | 160.3424 |

Raman profiles, ruling out the possibility of extended (tetrahedral-like) ordering for water in 1-octanol. This is also consistent with a destructuring effect induced by the confinement.

Insights into the IR and Raman spectral contributions due to segregated water can be obtained from ab initio calculations. Frequencies and activities of discrete water clusters such as open dimers, closed trimers, and tetramers (see Table 1) computed at the MP2 level are schematically displayed in Figure 9 as vertical segments. The position of each segment corresponds to the calculated wavenumber of the mode, while corresponding intensity or activity is reported on the vertical axis (values are intended positive also for the Raman side of the diagram). At a first glance, we observe a nice qualitative agreement between the calculated spectral lines and the IR/Raman experimental profiles. Our calculations show that an increase of cluster size results in both a frequency decrease and an activity increase (more strongly in IR than in Raman) of the bonded-OH stretching mode. On the other hand, free-OH vibrations are almost independent of the aggregation extent, as also indicated by the spectral evolution in Figure 8. It can be observed that the frequency position of the 3200 $cm^{-1}$ component of the IR profile is not fully reproduced by the considered water clusters. Therefore, species with higher coordination number (giving rise to lower frequency signals) than tetramer should be properly envisaged for a quantitative analysis.

Interesting similarities are observed between the profiles in Figures 8 and 9 and vibrational sum frequency (VSF) spectra[48] of *interfacial water*, suggesting the existence of comparable water arrangements. Specifically, two main features at approximately 3200 and 3400 $cm^{-1}$, along with sharp signals in the range 3600−3700 $cm^{-1}$, characterize the VSF profiles of water/vapor, water/$CCl_4$, and water/hexane interfaces.[49,50] In the description of these spectra, the component at 3200 $cm^{-1}$ is attributed to OHs of tetrahedrally coordinated water, for which intermolecular coupling is relevant,[51] the component at 3400 $cm^{-1}$ to uncoupled H-donor OHs, which form less and/or weak H-bonds, and the narrow signals near 3600−3700 $cm^{-1}$ to free-OH groups.[49,50,52] Therefore, the difference spectra that we obtained (Figures 8 and 9) can be safely attributed to saturating water; also, comparable aggregates are found between truly interfacial and confined water (at a mesoscopic scale), reinforcing the view of a microscopic heterogeneity in saturated 1-octanol at normal conditions.

At higher temperature (>180 °C), the MIR difference spectrum (Figure 8) reflects a consistent reduction in large water aggregates; essentially two components near 3550 and 3700 $cm^{-1}$ are observed, indicating the presence of respectively water dimers and monomers (see Figure 9). The broadening and blue-shift of the free-OH signal (having a maximum at 3640 $cm^{-1}$ for $T = 40$ °C, and at 3700 $cm^{-1}$ for $T = 300$ °C) can be related to the production of water monomers, with an antisymmetric stretching mode absorbing just at 3700 $cm^{-1}$.[49,50] This also supports the interpretation of NIR spectra given above. The component at 3550 $cm^{-1}$ can be attributed to the H-donor OH of single-bonded water molecules in water−water and/or water−alcohol dimers. It is worth noting that the signature of residual water clustering appears up to the highest temperature of the experiment. In the NIR spectra, the same evidence is provided by a relative red-shift and depletion of the signal at 7100 $cm^{-1}$ in the solution compared with the pure alcohol.

Therefore, water−octanol H-bonds in which water acts either as H-donor or acceptor toward free (terminal acceptor or monomeric) octanol molecules are found in this solution. The relevance of such bonding compared to water−water and alcohol−alcohol H-bond interactions appears to increase with the temperature, as the segregation vanishes. This seems to be consistent with findings from a recent NMR study of water−methanol mixtures.[53] Also, it has been shown for ethanol-rich aqueous mixtures that[54] the excess enthalpy of mixing is positive at high temperature, thus reflecting a relative decrease of attractive interactions in the mixture compared with the pure compounds. The prevalence of nonspecific interactions over H-bonds would then make the excess enthalpy go as expected for a regular mixture.[54] In the same way, a decrease of alcohol−alcohol hydrophobic interactions in wet 1-octanol at high temperature may explain the positive excess volume obtained here (see Figure 1).

Octanol−water H-bonds are thought to be essential in determining the peculiarities of the 1-octanol/water interface compared to other systems, namely 3-octanol/water and octane/water.[25−27] Such interface shows both a strongly H-bonding and low polarity character, this latter due to an alkane-like region with preferential orientation of the 1-octanol

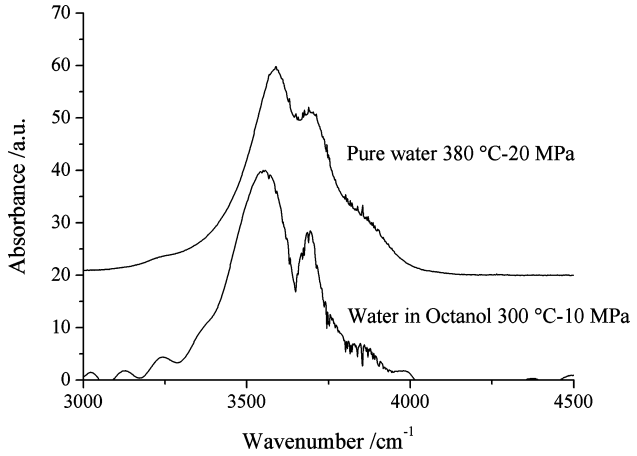


**Figure 10.** (Bottom to top) MIR spectrum of water in the water−octanol mixture at $T = 300$ °C and $P = 10$ MPa, compared to that of supercritical water at $T = 380$ °C and $P = 20$ MPa.[23,43]

molecules within the alcohol side of the boundary.[25] Strong water−1-octanol H-bonding at the interface is included in the bulk-like water network, without orientational preference of the H-bonded molecules therein.[26] The important role of interfacial water as both H-donor and acceptor in the H-bonding with octanol has also been remarked in the Monte Carlo simulation study of Jedlovszky et al.[27] In this case it is found that H-bonds between water and 1-octanol are preferentially aligned perpendicularly to the interface (in order to maximize the total number of H-bonds), with a fraction of ∼35% of bonded water molecules acting as acceptor in H-bonded species, in close analogy with our results. Moreover, an even larger percentage of H-donor water molecules is reported.[27] Hence, generally speaking, similar association properties can be found between water in wet octanol at high temperature and water at the interface with 1-octanol (at normal conditions). Note that the density of two immiscible liquids at the interface is considerably reduced with respect to the corresponding bulk values.[25−27]

Figure 10 shows the MIR difference profile obtained at the highest temperature of the experiment, along with a spectrum of pure supercritical water[23,43] (at $T = 380$ °C and $P = 20$ MPa). Under the applied supercritical conditions, authors could refer to the existence of essentially monomers and dimers of water.[43] This holds true even for water dispersed in octanol, although water−alcohol adducts are also expected to play a role. The poor compensation on the octanol free-OH signal (at 3640 $cm^{-1}$) is less pronounced here than in the NIR region (see Figure 4b) due to a reduced spectral intensity.

## 4. Conclusions

We studied the association of water-saturated 1-octanol by FTIR absorption spectroscopy in both NIR and MIR regions, from ambient temperature and pressure up to $T = 300$ °C and $P = 10$ MPa along the liquid−gas coexistence curve. Analysis of the difference spectra provided a molecular-level description of the H-bonding properties of hydrating water in the whole range of thermodynamic conditions applied. Two distinct regimes of association were determined through the spectral evolution as a function of temperature: at $T < 180$ °C, water is remarkably self-associated forming stable H-bonded clusters, while at higher temperature, monodispersed water along with small aggregates exist.

The spectra at low temperature reveal the existence of polar regions, with prevalent water−water interactions, giving rise to a microheterogeneous mixing. Signatures of a tetrahedral-like ordering for the segregated water were detected (up to 120 °C), although water is destructured compared to the bulk due to confinement constraints. Spectral patterns of segregated water in wet octanol recall the profiles of real water interfaces obtained by VSF spectroscopy.

Water association strongly reduces with the increase of temperature, while dimers and monomers become prevalent in the solution. Notably, H-bonded species still exist at the highest temperature investigated. Spectral features in the OH-stretching overtone profile reveal the role of water as proton-acceptor in H-bonded water−alcohol species, with around 30% of water molecules involved at 300 °C. Changes in the free-OH peak position additionally suggest the existence of mixed aggregates with proton-donor water molecules (this is also expected for statistical reasons because of the two OH bonds of water). On the whole, the importance of water−octanol H-bonds with respect to water−water and alcohol−alcohol ones is found to increase at higher temperature, when the overall aggregation is strongly depleted. These water−alcohol adducts are also essential in determining the molecular organization of the octanol/water interface at room temperature. Segregation effects are expected to vanish at higher temperature, as the density of the system shows significant deviations from the ideal behavior. The positive excess volume of mixing may indicate a water-induced decrease of attractive interactions around octanol molecules at high temperatures. In these conditions, the obtained spectra compare well with those of water in supercritical phase indicating that (besides water−alcohol aggregates) water monomers and water−water dimers characterize the state of water in wet octanol.

FTIR absorption spectroscopy in the regions of NIR and MIR, supported by quantum chemistry calculations of small water clusters, provided a molecular-level insight into the association properties of water in wet octanol within a broad range of thermodynamic conditions.

## References and Notes

(1) Leo, A.; Hansch, C.; Elkins, D. *Chem. Rev.* **1971**, *71*, 525.
(2) Martinez, M. N.; Amidon, G. L. *J. Clin. Pharmacol.* **2002**, *42*, 620.
(3) Debolt, S. E.; Kollman, P. A. *J. Am. Chem. Soc.* **1995**, *117*, 5316.
(4) Best, S. A.; Merz, K. M.; Reynolds, C. H. *J. Phys. Chem. B* **1999**, *103*, 714.
(5) MacCallum, J. L.; Tieleman, D. P. *J. Am. Chem. Soc.* **2002**, *124*, 15085.
(6) Chen, B.; Siepmann, J. I. *J. Phys. Chem. B* **2006**, *110*, 3555.
(7) Marcus, Y. *J. Solution Chem.* **1990**, *19*, 507.
(8) Franks, N. P.; Abraham, M. H.; Lieb, W. R. *J. Pharm. Sci.* **1993**, *82*, 466.
(9) Vahvaselka, K. S.; Serimaa, R.; Torkkeli, M. *J. Appl. Crystallogr.* **1995**, *28*, 189.
(10) Czarnecki, M. A. *J. Phys. Chem. A* **2000**, *104*, 6356.
(11) Sassi, P.; Marcelli, A.; Paolantoni, M.; Morresi, A.; Cataliotti, R. S. *J. Phys. Chem. A* **2003**, *107*, 6243.
(12) Sassi, P.; Morresi, A.; Paolantoni, M.; Cataliotti, R. S. *J. Mol. Liq.* **2002**, *96−7*, 363.
(13) Paolantoni, M.; Sassi, P.; Morresi, A.; Cataliotti, R. S. *Chem. Phys.* **2005**, *310*, 169.
(14) Sassi, P.; Paolantoni, M.; Cataliotti, R. S.; Palombo, F.; Morresi, A. *J. Phys. Chem. B* **2004**, *108*, 19557.
(15) Fileti, E. E.; Chaudhuri, P.; Canuto, S. *Chem. Phys. Lett.* **2004**, *400*, 494.
(16) Hu, K.; Zhou, Y.; Shen, J. F.; Ji, Z. P.; Cheng, G. Z. *J. Phys. Chem. B* **2007**, *111*, 10160.
(17) Bowron, D. T.; Moreno, S. D. *J. Chem. Phys.* **2002**, *117*, 3753.
(18) Sassi, P.; Paolantoni, M.; Perticaroli, S.; Palombo, F.; Morresi, A. *J. Raman Spectrosc.* **2009**, *40*, 1279.
(19) Dixit, S.; Crain, J.; Poon, W. C. K.; Finney, J. L.; Soper, A. K. *Nature* **2002**, *416*, 829.
(20) Dougan, L.; Hargreaves, R.; Bates, S. P.; Finney, J. L.; Reat, V.; Soper, A. K.; Crain, J. *J. Chem. Phys.* **2005**, *122*, 174514.

(21) Guo, J. H.; Luo, Y.; Augustsson, A.; Kashtanov, S.; Rubensson, J. E.; Shuh, D. K.; Agren, H.; Nordgren, J. *Phys. Rev. Lett.* **2003**, *91*, 4.
(22) Tomsic, M.; Jamnik, A.; Fritz-Popovski, G.; Glatter, O.; Vlcek, L. *J. Phys. Chem. B* **2007**, *111*, 1738.
(23) Tassaing, T.; Danten, Y.; Besnard, M. *J. Mol. Liq.* **2002**, *101*, 149.
(24) Palombo, F.; Tassaing, T.; Danten, Y.; Besnard, M. *J. Chem. Phys.* **2006**, *125*, 8.
(25) Napoleon, R. L.; Moore, P. B. *J. Phys. Chem. B* **2006**, *110*, 3666.
(26) Benjamin, I. *Chem. Phys. Lett.* **2004**, *393*, 453.
(27) Jedlovszky, P.; Varga, I.; Gilayi, T. *J. Chem. Phys.* **2004**, *120*, 11839.
(28) Rey, S. Ph.D. Thesis, University Bordeaux 1, 1999.
(29) Frisch, M. J.; Trucks, G. W.; Schlegel, H. B.; Scuseria, G. E.; Robb, M. A.; Cheeseman, J. R.; Montgomery, J. A., Jr.; Vreven, T.; Kudin, K. N.; Burant, J. C.; Millam, J. M.; Iyengar, S. S.; Tomasi, J.; Barone, V.; Mennucci, B.; Cossi, M.; Scalmani, G.; Rega, N.; Petersson, G. A.; Nakatsuji, H.; Hada, M.; Ehara, M.; Toyota, K.; Fukuda, R.; Hasegawa, J.; Ishida, M.; Nakajima, T.; Honda, Y.; Kitao, O.; Nakai, H.; Klene, M.; Li, X.; Knox, J. E.; Hratchian, H. P.; Cross, J. B.; Bakken, V.; Adamo, C.; Jaramillo, J.; Gomperts, R.; Stratmann, R. E.; Yazyev, O.; Austin, A. J.; Cammi, R.; Pomelli, C.; Ochterski, J. W.; Ayala, P. Y.; Morokuma, K.; Voth, G. A.; Salvador, P.; Dannenberg, J. J.; Zakrzewski, V. G.; Dapprich, S.; Daniels, A. D.; Strain, M. C.; Frakas, O.; Malick, D. K.; Rabuck, A. D.; Raghavachari, K.; Foresman, J. B.; Ortiz, J. V.; Cui, Q.; Baboul, A. G.; Clifford, S.; Cioslowski, J.; Stefanov, B. B.; Liu, G.; Liashenko, A.; Piskorz, P.; Komaromi, I.; Martin, R. L.; Fox, D. J.; Keith, T.; Al-Laham, M. A.; Peng, C. Y.; Nanayakkara, A.; Challacombe, M.; Gill, P. M. W.; Johnson, B.; Chen, W.; Wong, M. W.; Gonzales, C.; Pople, J. A. *Gaussian 03*, Revision C.02; Gaussian, Inc., Wallingford, CT, 2004.
(30) Xantheas, S. S.; Dunning, T. H. *J. Chem. Phys.* **1993**, *99*, 8774.
(31) Xantheas, S. S. *J. Chem. Phys.* **1995**, *102*, 4505.
(32) Oparin, R.; Tassaing, T.; Danten, Y.; Besnard, M. *J. Chem. Phys.* **2004**, *120*, 10691.
(33) Berti, P.; Cabani, S.; Mollica, V. *Fluid Phase Equilib.* **1987**, *32*, 195.
(34) Smith, B. D.; Srivastava, R. *Thermodynamic data for pure compounds*; Distributors for the U.S. and Canada, Elsevier Science Pub. Co.: Amsterdam, The Netherlands, and New York, NY, 1986.
(35) Wagner, W.; Pruss, A. *J. Phys. Chem. Ref. Data* **2002**, *31*, 387.
(36) Arce, A.; Blanco, A.; Soto, A.; Vidal, I. *J. Chem. Eng. Data* **1993**, *38*, 336.
(37) Bernazzani, L.; Cabani, S.; Conti, G.; Mollica, V. *J. Therm. Anal. Calorim.* **2000**, *61*, 637.
(38) Bazaev, A. R.; Abdulagatov, I. M.; Bazaev, E. A.; Abdurashidova, A. *J. Chem. Thermodyn.* **2007**, *39*, 385.
(39) Wojtkow, D.; Czarnecki, M. A. *J. Phys. Chem. A* **2005**, *109*, 8218.
(40) Wojtkow, D.; Czarnecki, M. A. *J. Phys. Chem. A* **2006**, *110*, 10552.
(41) Palombo, F.; Paolantoni, M.; Sassi, P.; Morresi, A.; Cataliotti, R. S. *J. Mol. Liq.* **2006**, *125*, 139.
(42) Oparin, R.; Tassaing, T.; Danten, Y.; Besnard, M. *J. Chem. Phys.* **2005**, *122*, 8.
(43) Tassaing, T.; Garrain, P. A.; Baraille, I.; Bégué, D. *J. Chem. Phys.* **2010**, in press.
(44) Danten, Y.; Tassaing, T.; Besnard, M. *J. Phys. Chem. A* **2000**, *104*, 9415.
(45) Paolantoni, M.; Lago, N. F.; Alberti, M.; Lagana, A. *J. Phys. Chem. A* **2009**, *113*, 15100.
(46) Besnard, M.; Danten, Y.; Tassaing, T. *J. Chem. Phys.* **2000**, *113*, 3741.
(47) Torii, H. *J. Phys. Chem. A* **2006**, *110*, 9469.
(48) McFearin, C. L.; Beaman, D. K.; Moore, F. G.; Richmond, G. L. *J. Phys. Chem. C* **2009**, *113*, 1171.
(49) Scatena, L. F.; Brown, M. G.; Richmond, G. L. *Science* **2001**, *292*, 908.
(50) Scatena, L. F.; Richmond, G. L. *J. Phys. Chem. B* **2001**, *105*, 11240.
(51) Auer, B. M.; Skinner, J. L. *J. Phys. Chem. B* **2009**, *113*, 4125.
(52) Raymond, E. A.; Tarbuck, T. L.; Brown, M. G.; Richmond, G. L. *J. Phys. Chem. B* **2003**, *107*, 546.
(53) Corsaro, C.; Spooren, J.; Branca, C.; Leone, N.; Broccio, M.; Kim, C.; Chen, S. H.; Stanley, H. E.; Mallamace, F. *J. Phys. Chem. B* **2008**, *112*, 10449.
(54) Larkin, J. A. *J. Chem. Thermodyn.* **1975**, *7*, 137.
(55) Scott, A. P.; Radom, L. *J. Phys. Chem.* **1996**, *100*, 16502.

JP1009548